Imaging techniques through discrete scattering media by polarized pulse waves

Sermsak Jaruwatanadilok, Akira Ishimaru, and Yasuo Kuga

Department of Electrical Engineering, University of Washington, Seattle, WA, USA

ABSTRACT

Imaging through random media is an important problem with many applications including optical remote sensing and bio-optics. As the optical depth gets larger, the imaging resolution and contrast deteriorates because of the effect of scattering. In this paper, we present the solution to the vector radiative transfer equation (VRTE) and its application to the optical imaging problem. Since the incoherent component created by the scattering in random media is responsible for the deterioration of the quality of images, several techniques are proposed to improve the imaging by reducing the incoherent component. Off-Axis Intensity Subtraction (OAIS) and Cross-Polarization Intensity Subtraction (CPIS) imaging technique are based on the fact that off-axis and cross polarization contains most of the incoherent component. Photon Density Waves (PDW) is a frequency-domain method which exhibits less effect of multiple scattering from the random media. We investigate the techniques mentioned above using numerical solution of VRTE and show the effectiveness, the limitations and the conditions of these techniques. Because we consider the polarized pulse waves case, we also discussed in the time-domain behavior and the application of time-gating to the imaging problem. The time-gating method is investigated in both position and duration. Since in practice an array of detectors are often used, we also include the effect of Field Of View of a detector (pixel FOV) in our calculations. We quantitatively measure the performance of imaging techniques by contrast. Also, we apply these techniques to numerical simulations of cross images and show the improvement of the quality of the images.

Keywords: radiative transfer, multiple scattering, polarized pulse waves, optical imaging, photon density waves

1. INTRODUCTION

Imaging through discrete scattering media has been a challenging problem for long time. Discrete scattering media are very common in real world scenarios. Examples are fog and clouds in the optical remote sensing and atmospheric applications, and tissue and blood in the bio-optics applications. The solution to the scattered waves can be treated by the Maxwell equation. However, the solution is rigurous and required a lot of computation. A more attractive alternative is the radiative transfer equation.[1] Although the radiative transfer equation does not include the phase of the wave, it contains the polarization information.

It is well-known that the scattering from the discrete random media creates the blurring of the image[2,3]. Therefore, to improve the imaging, several techniques are applied in order to reduce the scattering effect. The Off-Axis Intensity Subtraction (OAIS) is based on the assumption that the diffused component is mostly off-axis.[4] Thus, subtracting the off-axis intensity should reduce the scattering effect. However, this technique requires at least an additional receiver which might be inconvenient in some applications. The Cross-Polarization Intensity Subtraction (CPIS) technique uses the cross-polarized component to subtract off the co-polarized component. Photon Density Waves is another technique using frequency modulation which exhibit less scattering effect[5−9] . We study the polarized pulse wave because it adds one more control variable to the imaging.[10] We investigate the time gating effect to the quality of the image. We show the both the position and the duration of the time gating are important factors. We also discuss the field of view (FOV) effect from the receivers. The field of view dictates the amount of diffuse component captured by the imaging system.

Further author information: (Send correspondence to Sermsak Jaruwatanadilok)
Department of Electrical Engineering, Box 352500, University of Washington, Seattle, WA, 98195; Phone: (206) 543-2159; E-mail: sermsak@ee.washington.edu

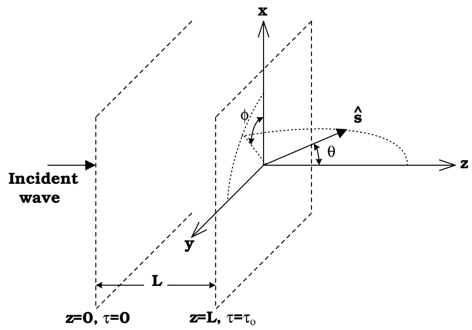

Figure 1. Plane-parallel problem.

In this paper, we derive the pulse vector radiative transfer equation and its solutions in the plane-parallel medium in section 2. Based on the radiative transfer theory, we study the behavior of light through the random medium by calculating the Stokes vector. Next, we explain the imaging formulation through a random medium by an imaging system in section 3. We also investigate several techniques used to improve the image quality which are Off-Axis Intensity Subtraction (OAIS), Cross-Polarization Intensity Subtraction (CPIS), and the Photon Density Wave (PDW). Time domain behavior of the light suggests that time-gating should improve quality of images. As a result, we investigate the effect of time-gating to the imaging in section 4. In this section, we also discuss the effect of the pixel field of view (FOV). Finally we conclude in section 5.

2. VECTOR RADIATIVE TRANSFER EQUATION

We consider a plane wave propagating through a slab of random medium of thickness L in a plane-parallel geometry shown in figure 1. Here, the random media is defined as randomly located dielectric spheres suspended in a homogeneous background. We study the modified Stokes vector which explains the intensity and the polarization state of the wave. The equation that explains the modified Stoke parameters through this random medium in both time and space domain is the narrow-band, time-dependent vector radiative transfer equation expressed by

$$\left(\mu\frac{\partial}{\partial z}+\rho\sigma_t+\frac{1}{c}\frac{\partial}{\partial t}\right)\mathbf{I}(t,z,\mu,\phi)=\int_0^{2\pi}\int_{-1}^{1}\mathbf{S}(\mu,\phi,\mu',\phi')\mathbf{I}(t,z,\mu',\phi')\,\mu'\,\phi' \\ +\mathbf{J}(t,z,\mu,\phi),\ \text{for } 0\leq z\leq L \tag{1}$$

where $\mu=\cos\theta$, ρ is the number density, σ_t is the total scattering of a single particle, c is the speed of the wave in the medium. The modified Stokes vector $\mathbf{I}$ is defined by

$$\mathbf{I}=\begin{bmatrix}I_1 & I_2 & U & V\end{bmatrix}^T \tag{2}$$

where T denotes the transpose operator of a matrix. The Mueller matrix $\mathbf{S}$ is explained in.[11] It characterizes the scattering behavior of the random media. The source term is denoted by $\mathbf{J}$.

To make the equation easier to handle, we normalize the space domain with $\rho\sigma_t$ and the time domain with L/c. Thus, equation (1) becomes

$$\left(\mu\frac{\partial}{\partial \tau}+1+\frac{1}{\tau_o}\frac{\partial}{\partial t_n}\right)\mathbf{I}(t_n,\tau,\mu,\phi)=\int_0^{2\pi}\int_{-1}^{1}\mathbf{S}(\mu,\phi,\mu',\phi')\mathbf{I}(t_n,\tau,\mu',\phi')\,\mu'\,\phi' \\ +\mathbf{J}(t_n,\tau,\mu,\phi),\ \text{for } 0\leq \tau\leq \tau_o \tag{3}$$

where $\tau=\rho\sigma_t z$ is the *optical distance*, $\tau_o=\rho\sigma_t L$ is the *optical depth*, and $t_n=t\,(L/c)^{-1}$ is the normalized time. For convenience, we omit the subscript n and denote t as the normalized time. To make the total intensity a positive quantity, the photon density wave consists of the constant term and the time-dependent term, i.e.

$$\mathbf{I}_{total}(t) = \mathbf{I}_{constant} + \mathbf{I}(t)\exp(-i\omega_{mod}t) \tag{4}$$

where $\omega_{mod} = 2\pi f_{mod}$, and f_{mod} is the modulation frequency. We only consider the time-dependent term in our development. Our derivation is for the generalized case including the photon density waves. In the regular pulse wave case, the modulation frequency is set to zero.

For ease of calculations, the modified Stokes vector is often divided into two parts: the reduced intensity (coherent) modified Stokes vector and the diffuse (incoherent) modified Stokes vector. The reduced intensity modified Stokes vector is the component that decreases due to the scattering and absorption from the particles. It satisfies the equation

$$\frac{\partial}{\partial\tau}\mathbf{I}_{ri} = -\mathbf{I}_{ri} \tag{5}$$

where $\mathbf{I}_{ri}$ denotes the reduced intensity modified Stokes vector. In the plane wave case, it is expressed as

$$\mathbf{I}_{ri}(t,\tau) = \mathbf{I_o} f(t,\tau)\exp(-\tau)\delta(\phi)\delta(\mu-1). \tag{6}$$

$\mathbf{I_o}$ is the incident modified Stokes vector. We consider two cases of incident waves. For linear polarization in the x direction, the incident modified Stokes vector is

$$\mathbf{I_o} = \begin{bmatrix}1 & 0 & 0 & 0\end{bmatrix}^T \tag{7}$$

and for left-handed circular polarization, it is

$$\mathbf{I_o} = \begin{bmatrix}1/2 & 1/2 & 0 & 1\end{bmatrix}^T. \tag{8}$$

The pulse shape function for the photon density waves $f(t,\tau)$ is defined as

$$f(t,\tau) = \begin{cases} \exp\left[-i\omega_m\left(t-\dfrac{\tau}{\tau_o}\right)\right] & \text{for continuous wave} \\ \delta\left(t-\dfrac{\tau}{\tau_o}\right)\exp\left[-i\omega_m\left(t-\dfrac{\tau}{\tau_o}\right)\right] & \text{for delta function pulse} \\ \dfrac{1}{\sqrt{\pi}\,T_o}\exp\left[-\dfrac{(t-\tau/\tau_o)^2}{T_o^2} - i\omega_m\left(t-\dfrac{\tau}{\tau_o}\right)\right] & \text{for Gaussian pulse} \end{cases} \tag{9}$$

where $\omega_m = \omega_{mod}(L/c)$ is the normalized angular modulation frequency and T_o is the pulse width in the Gaussian pulse wave case.

Another component, the diffuse modified Stokes vector $\mathbf{I}_d$, satisfies the equation

$$\left(\mu\frac{\partial}{\partial\tau} + 1 + \frac{1}{\tau_o}\frac{\partial}{\partial t}\right)\mathbf{I}_d(t,\tau,\mu,\phi) = \int_0^{2\pi}\int_{-1}^{1}\mathbf{S}(\mu,\phi,\mu',\phi')\mathbf{I}_d(t,\tau,\mu',\phi')\,\mu'\,\phi' + \mathbf{E}_{ri}(t,\tau,\mu,\phi), \text{ for } 0 \le \tau \le \tau_o. \tag{10}$$

In our calculations, we assume a source-free medium. Thus, the source term $\mathbf{J}$ only has the contribution from the incident wave. It is defined as the equivalent source term $\mathbf{E}_{ri}$, given by

$$\begin{aligned}\mathbf{E}_{ri} &= \textstyle\int_0^{2\pi}\int_{-1}^{1}\mathbf{S}(\mu,\phi,\mu',\phi')\mathbf{I}_{ri}(t,\tau,\mu',\phi')\,\mu'\,\phi' \\ &= \mathbf{F_o}(\mu,\phi)f(t,\tau)\exp(-\tau)\end{aligned} \tag{11}$$

where $\mathbf{F_o}(\mu,\phi) = \mathbf{S}(\mu,\phi 1,0)\mathbf{I_o}$.

To be able to solve equation (10), we use the Fourier transform to obtain the frequency-domain vector radiative transfer equation expressed as

$$\left(\mu\frac{\partial}{\partial\tau} + 1 - i\frac{\omega}{\tau_o}\right)\mathbf{I}_d(\omega,\tau,\mu,\phi) = \int_0^{2\pi}\int_{-1}^{1}\mathbf{S}(\mu,\phi,\mu',\phi')\mathbf{I}_d(\omega,\tau,\mu',\phi')\,\mu'\,\phi' + \mathbf{F_o}(\mu,\phi)f(\omega,\tau)\exp(-\tau), \text{ for } 0 \le \tau \le \tau_o \tag{12}$$

where

$$\mathbf{I}_d(\omega,\tau,\mu,\phi) = \int \mathbf{I}_d(t,\tau,\mu,\phi)\exp(i\omega t)\, t. \tag{13}$$

ω is the normalized angular frequency, and the pulse shape function in the frequency domain is given by

$$f(\omega,\tau) = \int f(t,\tau)\exp(i\omega t)\mathrm{d}t. \tag{14}$$

Then, the pulse shape function in equation (9) becomes

$$f(\omega,\tau) = \begin{cases} \exp\left(-i\omega\dfrac{\tau}{\tau_o}\right) 2\pi\delta(\omega-\omega_m) & \text{for continuous wave} \\ \exp\left(-i\omega\dfrac{\tau}{\tau_o}\right) & \text{for delta function pulse} \\ \exp\left(-i\omega\dfrac{\tau}{\tau_o}\right)\exp\left[-\dfrac{(\omega-\omega_m)^2 T_o^2}{4}\right] & \text{for Gaussian pulse.} \end{cases} \tag{15}$$

Let $\omega = \omega_m + \omega'$ and $\mathbf{I'}_d(\omega,\tau) = \mathbf{I}_d(\omega,\tau)\exp(-i\omega\tau/\tau_o)$, equation (12) becomes

$$\begin{aligned} &\left[\mu\frac{\partial}{\partial\tau} + 1 + (\mu-1)i\frac{\omega'+\omega_m}{\tau_o}\right]\mathbf{I'}_d(\omega',\tau,\mu,\phi) \\ &= \int_0^{2\pi}\int_{-1}^{1}\mathbf{S}(\mu,\phi,\mu',\phi')\mathbf{I'}_d(\omega',\tau,\mu',\phi')\,\mu'\,\phi' \\ &\quad +\mathbf{F_o}(\mu,\phi)f(\omega',\tau)\exp(-\tau),\ \text{for } 0\le\tau\le\tau_o \end{aligned} \tag{16}$$

where

$$f(\omega',\tau) = \begin{cases} 2\pi\delta(\omega') & \text{for continuous wave} \\ 1 & \text{for delta function pulse} \\ \exp\left(-\dfrac{\omega'^2 T_o^2}{4}\right) & \text{for Gaussian pulse.} \end{cases} \tag{17}$$

Equation (16) is in a much simpler form to solve. It also eliminates the instability caused by the high frequency component in the function $f(\omega,\tau)$. We solve this equation by imposing the boundary conditions given by

$$\mathbf{I'}_d(\tau=0) = 0 \quad \text{for} \quad 0\le\mu\le 1 \tag{18}$$

$$\mathbf{I'}_d(\tau=\tau_o) = 0 \quad \text{for} \quad -1\le\mu\le 0. \tag{19}$$

After solving equation (16), we have the diffuse modified Stokes vector in the frequency domain. We can obtain the time-domain diffuse modified Stokes vector by

$$\mathbf{I}_d(t,\tau) = \frac{1}{2\pi}\int \mathbf{I'}_d(\omega',\tau)\exp\left(i\omega\frac{\tau}{\tau_o} - i\omega' t\right)\omega'. \tag{20}$$

To solve equation (16), we expand the specific intensity in Fourier series in the azimuthal (ϕ) domain. A detailed explanation is presented in our previous works.[11] For linear polarization, the specific intensity is non-zero in mode zero and mode two, and for circular polarization, it is non zero only in mode zero. We also integrate the Mueller matrix with respect to the azimuthal dependence as expressed as

$$\mathbf{L}(\mu,\mu') = \int_0^{2\pi}\mathbf{S}(\mu,\mu',\phi'-\phi)\,(\phi'-\phi). \tag{21}$$

In the case of the delta function pulse, equation (16) reduces to

$$\begin{aligned} &\mu\frac{\partial}{\partial\tau}\mathbf{I'}_d(\omega',\tau,\mu) + \left[1 + (\mu-1)i\frac{\omega'+\omega_m}{\tau_o}\right]\mathbf{I'}_d(\omega,\tau,\mu) \\ &= \int_{-1}^{1}\mathbf{L}(\mu,\mu')\mathbf{I'}_d(\omega',\tau,\mu')\,\mu' + \mathbf{F_o}(\mu)\exp(-\tau),\ \text{for } 0\le\tau\le\tau_o. \end{aligned} \tag{22}$$

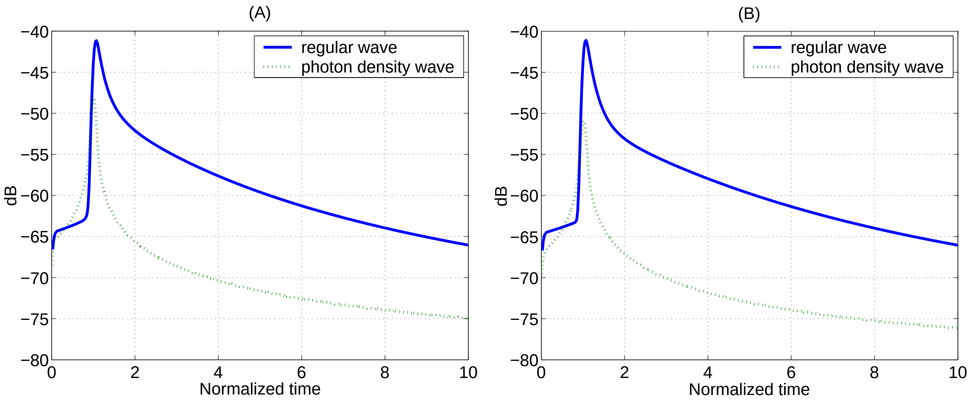

Figure 2. Forward pulse CW wave and 10 MHz photon density wave (0.68^o) as a function of time (A) Circular polarization and (B) Linear polarization.

By applying the Gauss quadrature formula[12] of order N in μ dependent to equation (16), we obtain a first-order differential equation in the form of

$$\frac{\partial}{\partial\tau}\mathbf{I}+\mathbf{A}\mathbf{I}=\mathbf{B}\exp(-\tau) \tag{23}$$

where

$$\mathbf{I}=\left[\mathbf{I'}_d(\omega',\tau,\mu_{-N}) \quad \cdots \quad \mathbf{I'}_d(\omega',\tau,\mu_N)\right]^T \tag{24}$$

$$\mathbf{A}_{j,k}=\frac{1}{\mu_j}\left[1+(\mu_j-1)i\frac{\omega'+\omega_m}{\tau_o}\right]-\frac{\mathbf{L}(\mu_j,\mu_k)}{\mu_j} \tag{25}$$

$$\mathbf{B}_{j,k}=\frac{\mathbf{F_o}(\mu_j)}{\mu_j}. \tag{26}$$

The solution to equation (23) consists of the particular solution and the complementary solution. By imposing the boundary conditions in equation (18) and (19), we can find the complete solution. We separately solve equation (16) for linear and circular polarizations. In the linear polarization case, only mode zero and mode two are non-zero, and in the circular polarization case only mode zero is non-zero. We use a wavelength of 1 micron. The random medium is fog particles, assumed to be spheres of water, with size distributions shown in table 1 suspended in the air. Therefore, the Mueller matrix can be calculated based on Mie solution.[13] The path length of the medium (L) is 1 km. The concentration of fog particles is varied according to the optical depth. For linear polarization, the co-polarized component in the forward direction is in the x direction and the cross-polarized component is in the y direction. On the other hand, for circular polarization, the co-polarized component in the forward direction is left-handed and the cross-polarized component is right-handed.

Table 1. Particle size distribution of fog.

	Distribution							
Diameter of Particle (μm)	0.4	0.6	0.7	1.4	2.0	3.6	5.4	8.0
Number of particles	3	10	40	50	7	1	9	2

We calculate the pulse wave and pulse photon density wave through a random medium. As the results show in figure 2 , the photon density waves show much lesser pulse broadening which is the effect from scattering.

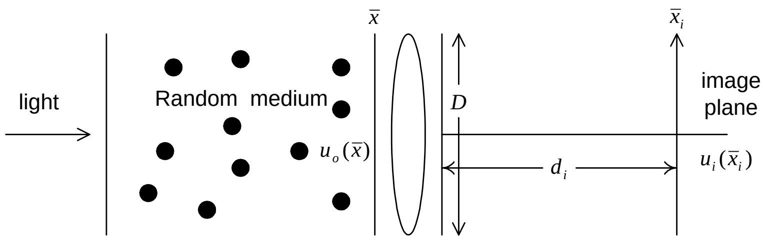

Figure 3. An imaging system.

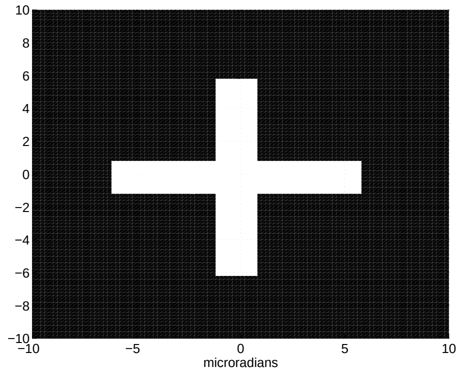

Figure 4. A cross image.

3. IMAGING SYSTEM AND TECHNIQUES TO IMPROVE IMAGE QUALITY

Fig. 3 shows the diagram of a simple imaging system that we used for our analysis. The circular lens has a diameter of D with a focal distance of d_i. The intensity at the image plane is given by

$$I_i(\bar{s}_i) = \frac{k^2}{(2\pi d_i)^2}(\pi a^2)^2 \left\{ \exp(-\tau_o) \left[\frac{J_1(ks_i a)}{(ks_i a/2)} \right]^2 + \frac{1}{\pi} \left(\frac{\lambda}{a} \right)^2 I_{inc}(\bar{s}_i) \right\} \tag{27}$$

where J_1 is the Bessel function of the first order, a is the radius of the aperture, $s_i = \sin\theta$, and I_{inc} is the incoherent intensity calculated from the radiative transfer equation explained in the previous section. To be able to compare with the other techniques, we define the contrast as

$$C = \frac{I_{i-coh}(s_i = 0) - I_{i-inc}(s_i = 0)}{I_{i-coh}(s_i = 0)}. \tag{28}$$

Different techniques are proposed to improve imaging through random media. They are based on the assumption that the scattering effect from random media creates background noise that impairs the contrast of the images. The off-axis intensity subtraction (OAIS) and cross-polarization intensity subtraction (CPIS) methods are believed to help alleviate the effect from scattering. OAIS is based on the assumption that the off-axis component of the wave comes from scattering and CPIS is based on the assumption that the cross-polarized component of the wave is the result of the scattering. On the other hand, photon density wave characteristics show that they are less influenced by the scattering of random media. Thus, using photon density wave could produce better images.

A cross pattern shown in figure 4 is imaged through random media. The angular size of a cross extends from -10 to 10 microradians. The circular lens has a 1 meter aperture size (D) and the wavelength is 1 micron.

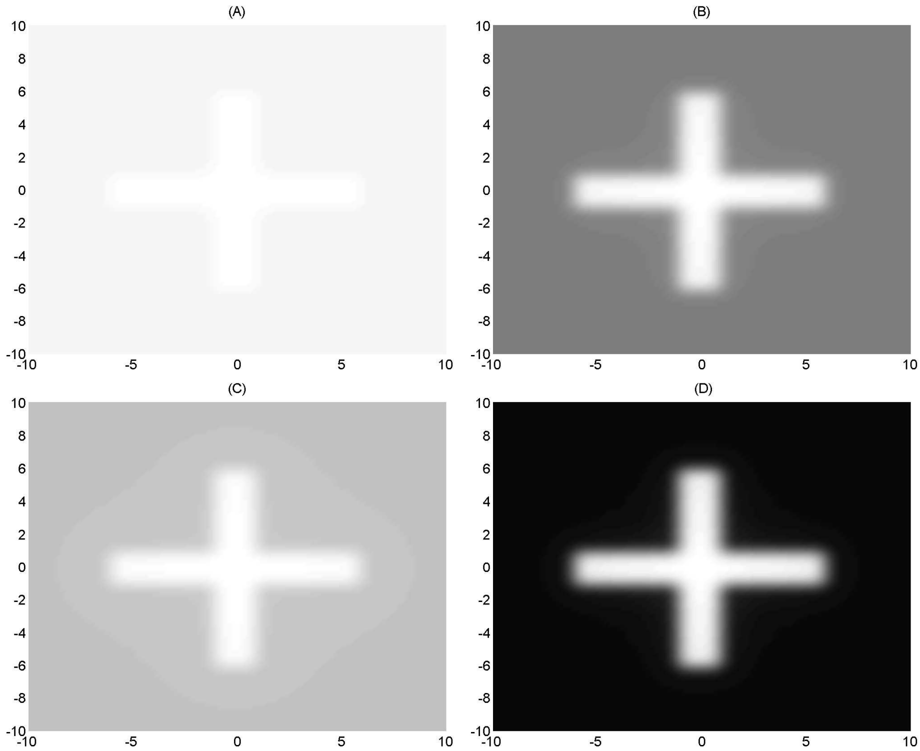

Figure 5. The circular polarized cross images through random media of optical depth 30 using (A) co-polarized wave, (B) CPIS, (C)OAIS, and (D) 1 MHz photon density waves. The angular sizes are in microradians.

Table 2. Contrast of the cross images.

	Optical depth=30	
	CP	LP
Co-pol	0.7429	0.7730
CPIS	38.5695	171.3048
OAIS	10.6032	10.9085
1 MHz PWD	1093.9780	1011.2420

The random medium in this case is fog particles in an air background explained previously. The path length of the random medium is 1 km. The number density of particles is adjusted to give an optical depth of 30. The images obtained using different techniques are shown in figures 5 and 6 in the circular polarization and linear polarization cases, respectively.

Table 2 lists the contrast of these images using equation (28) in the case of optical depth 30. From the results, it appears that the photon density waves visually give better images and perform better in term of contrast which corresponds to the calculated contrast.

4. TIME GATING AND FIELD OF VIEW EFFECT

We investigate the effect of time-gating and field of view of the receivers to the quality of images. First we study the effect of the field of view. We calculate the cross imaging using the field of view of 1 and 5 microradians

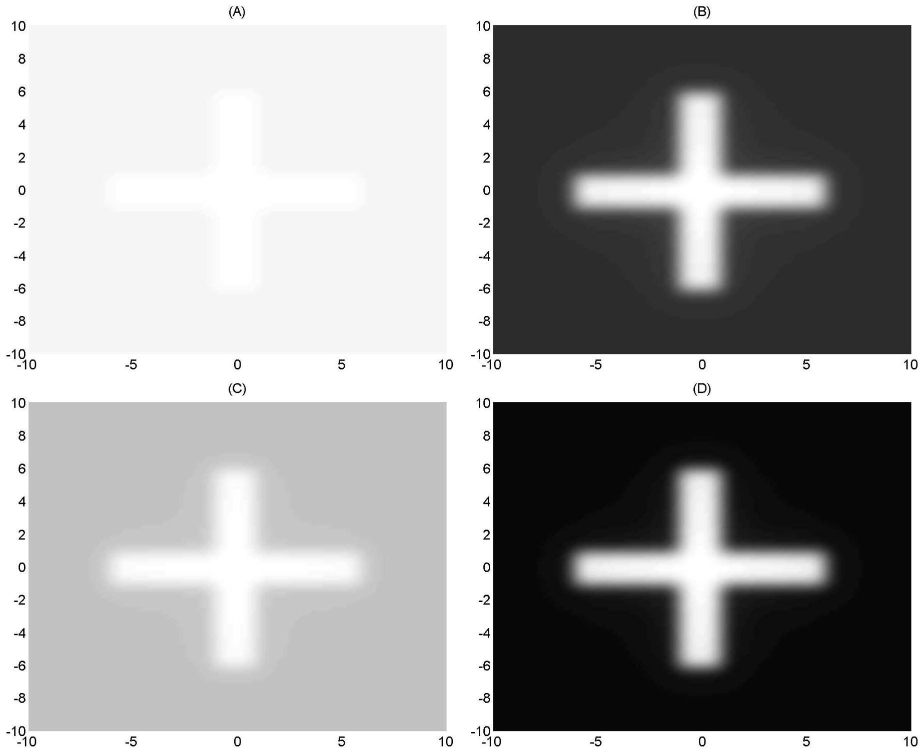

Figure 6. The linear polarized cross images through random media of optical depth 30 using (A) co-polarized wave, (B) CPIS, (C)OAIS, and (D) 1 MHz photon density waves. The angular sizes are in microradians.

with several techniques explained in the previous section. The results are illustrated in figure 7. It shows that the larger field of view makes the image more blurred because of the intensity averaging.

When polarized pulse waves are used, we can control the time-gating of the imaging. We investigate the effect of the duration of time-gating to the quality of the images. The results are shown in figure 8. The results confirm that the shorter the time-gating, the better the images. It is because the shorter the time-gating, the lesser the incoherent component coming from the scattering. It is important that the time-gating should include the coherent pulse as much as possible because the coherent component contributes to the high resolution imaging. From the results, we can conclude that the best image comes from shorter time-gating with smaller receiver field of view. However, field of view characteristic of the receivers is physical and cannot be changed in a particular imaging system unless the receivers are changed themselves. The parameter that we can control is the time-gating through shuttering and or signal processing.

5. CONCLUSIONS

We derive the generalized pulse vector radiative transfer equation in order to calculate the diffuse component of light propagating through discrete random media. Our derivation also includes the photon density waves calculation. We show that the photon density waves exhibit less scattering effect from the random media. In addition, we illustrate several techniques to improve imaging which are OAIS, CPIS, and photon density wave techniques. Photon density wave technique provide the best improvement in term of contrast. We examine the effect of the field of view of the receivers to the imaging. As the field of view gets larger, the resolution of the image is coarser. In case of pulse imaging, we investigate the time-gating. We find that the shorter time-gating, the smaller amount of diffuse component is captured, and the better the images. The best combination for better imaging is to have short time-gating, small field of view, and applying the photon density wave.

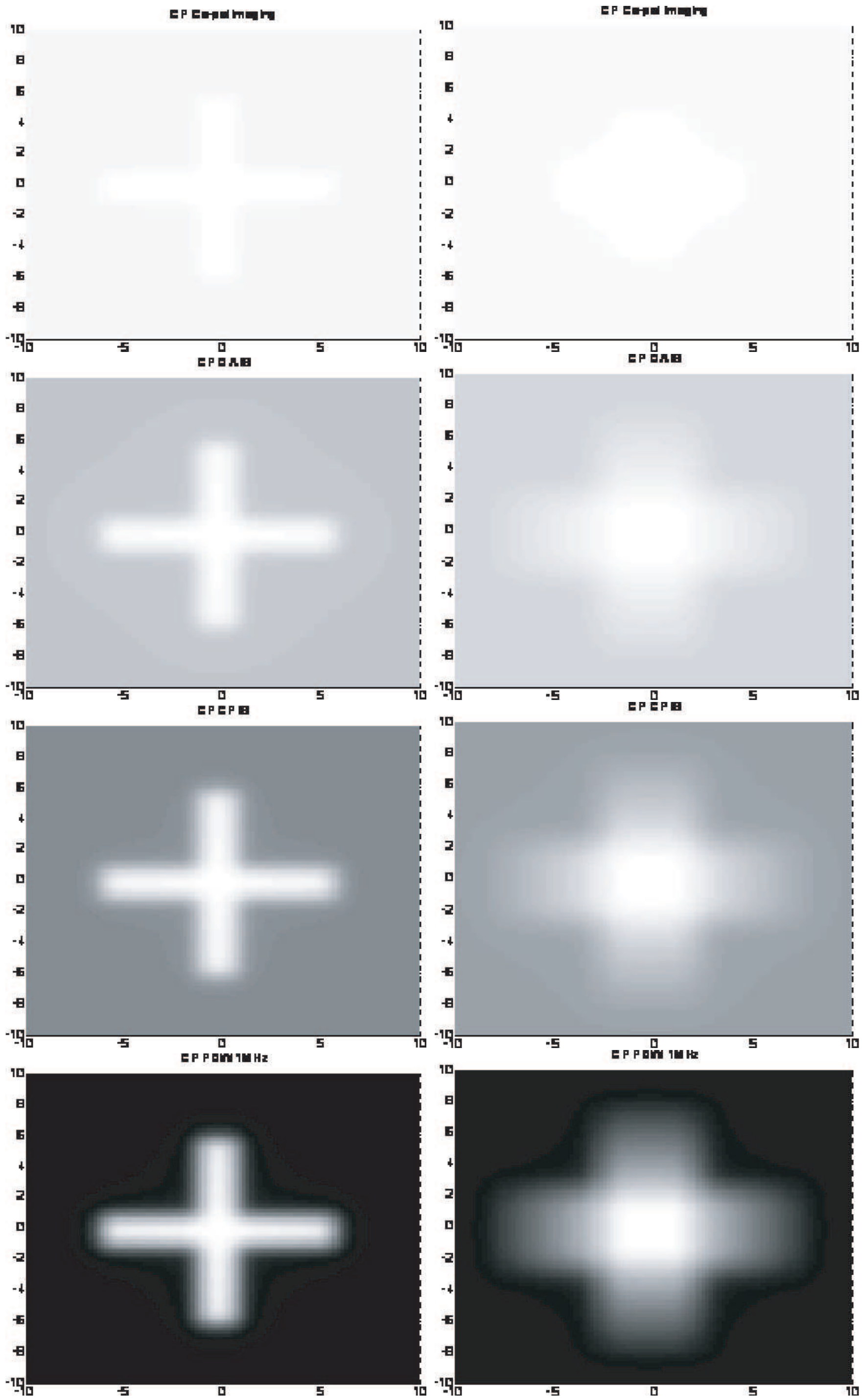

Figure 7. Field of view effect to CW imaging. Left column shows FOV of 1 microradian and right column shows FOV of 5 microradians. Top row is co-polarized imaging, second row is OAIS, third row is CPIS, and bottom row is photon density waves

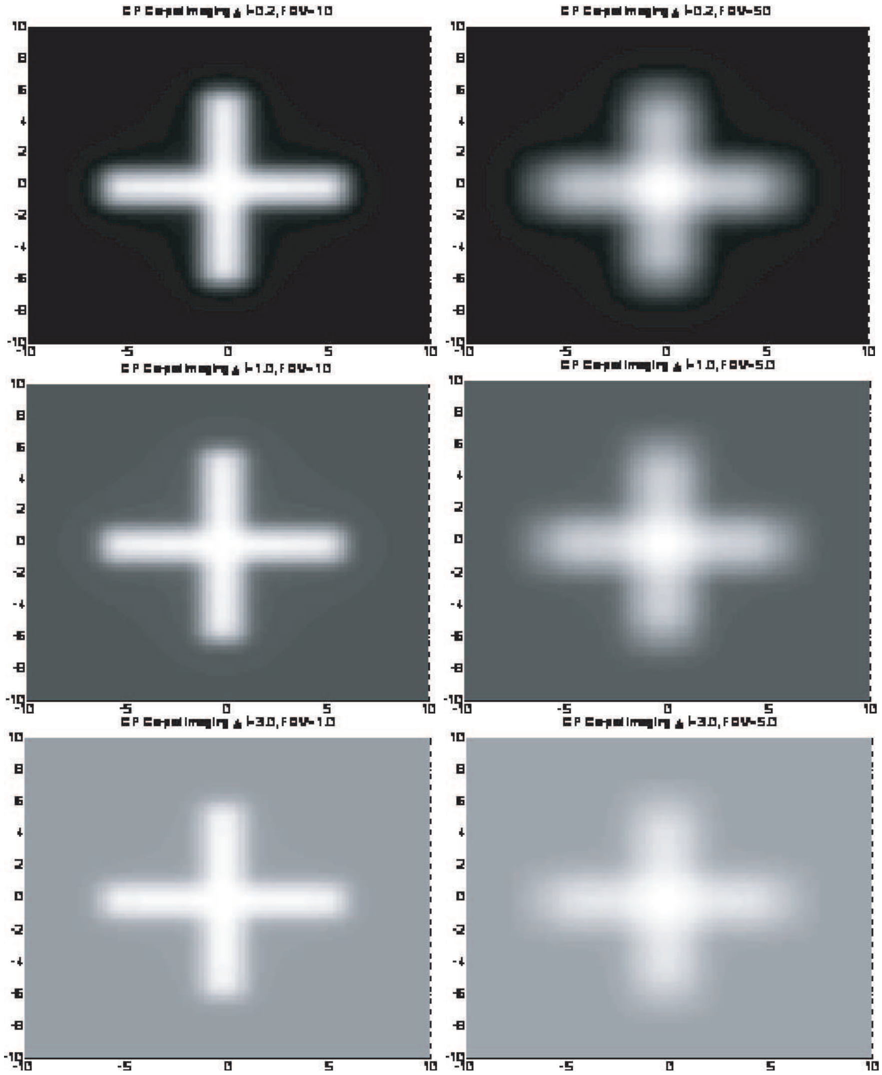

Figure 8. Field of view effect to CW imaging. Left column shows FOV of 1 microradian and right column shows FOV of 5 microradians. Top row is time-gating is 0.2, second row is time-gating of 1, and the bottom row is time-gating of 3. The time unit is normalized to L/c

ACKNOWLEDGMENTS

This work is supported by the National Science Foundation (grant ECS-9908849) , the Office of Naval Research (grant N000140010027) and the U.S. Air Force Research Laboratory (grant F29601-00-C-0240). We thank Charles Matson, U.S. Air Force Research laboratory, for many discussions, comments, and suggestions.

REFERENCES

1. S. Chandrasekhar, *Radiative Transfer*, Dover, New York, 1960.
2. A. Ishimaru, "Limitation on image resolution imposed by a random medium," *Applied Optics* **17**, pp. 384–352, 1978.
3. Y. Kuga and A. Ishimaru, "Modulation transfer function and image transmission through randomly distributed spherical particles," *Journal of the Optical Society of America A (Optics and Image Science)* **2**(12), pp. 2330–6, 1985.
4. K. Shimizu and M. Kitama, "Fundamental study on near-axis scattered light and its application to optical computed tomography,"
5. S. Fantini and E. Gratton, "Fluorescence photon-density waves in optically diffusive media," *Optics Communications* **173**(1-6), pp. 73–9, 2000.
6. L. Mullen, G. Yang, and V. M. Contarino, "Modulated pulse lidar system for water frequency spectra measurements," in *Conference on Lasers and Electro-Optics*, **6**, pp. 403–4, (Washington, DC, USA), 1998.
7. L. J. Mullen and V. M. Contarino, *Hybrid LIDAR-RADAR: seeing through the scatter*, vol. 1 of *IEEE Microwave Magazine*, 2000.
8. J. B. Fishkin, S. Fantini, M. J. vandeVen, and E. Gratton, "Gigahertz photon density waves in a turbid medium: theory and experiments," *Physical Review E (Statistical Physics, Plasmas, Fluids, and Related Interdisciplinary Topics)* **53**(3), pp. 2307–19, 1996.
9. B. J. Tromberg, L. O. Svaasand, T. T. Tsong, and R. C. Haskell, "Properties of photon density waves in multiple-scattering media," *Applied Optics* **32**(4), pp. 607–16, 1993.
10. P. Bruscaglioni, G. Zaccanti, and Q. Wei, "Transmission of a pulsed polarized light beam through thick turbid media: numerical results," *Applied Optics* **32**(30), pp. 6142–6150, 1993.
11. A. Ishimaru, S. Jaruwatanadilok, and Y. Kuga, "Polarized pulse waves in random discrete scatterers," *Applied Optics* **40**(30), pp. 5495–502, 2001.
12. A. Ishimaru, *Wave Propagation and Scattering in Random Media*, IEEE, New York, 1997.
13. H. C. Van de Hulst, *Light Scattering by Small Particles*, Dover, New York, 1957.